Bactericidal Activity of a Ce-Promoted Ag/AlPO4 Catalyst Using Molecular Oxygen in Water

QINGYUN CHANG,[†] HONG HE,*[,†] JINCAI ZHAO,[‡] MIN YANG,[†] AND JIUHUI QU[†]

Research Center for Eco-Environmental Sciences, Chinese Academy of Sciences, Beijing 100080, China, and Institute of Chemistry, Chinese Academy of Sciences, Beijing 100085 China

Received July 21, 2007. Revised manuscript received November 19, 2007. Accepted December 4, 2007.

The catalytic inactivation of *Escherichia coli* in water by a cerium (Ce)-promoted silver-loaded aluminum phosphate (Ag/$AlPO_4$) catalyst using molecular oxygen was investigated. With optimum Ce content, the Ag(Ce)/$AlPO_4$ catalyst exhibited strong bactericidal activity. The process of decomposition of the cell wall and cell membrane was directly observed by TEM. The different morphological changes of *E. coli* cells treated with the Ag(Ce)/$AlPO_4$ catalyst and those treated with Ag^+ suggested that the Ag^+ eluted from the catalyst surface did not play an important role during the bactericidal process. Results of DMPO spin-trapping measurements by electron spin resonance (ESR) indicated the formation of the reactive oxygen species (ROS) •OH and $•O_2^-$, which caused the considerable bactericidal activity. The formation of H_2O_2 acted as an important intermediate; this was confirmed by addition of catalase as the scavenger. A possible catalytic oxidation bactericidal mechanism using molecular oxygen was proposed for the Ag(Ce)/$AlPO_4$ catalyst.

Introduction

Pathogenic microbes are contaminants of major concern in drinking water, thus disinfection of water is very important to provide a sanitary environment and maintain human health. However, the commonly used disinfection methods, such as chlorination, ozonation,and ultraviolet (UV) irradiation, have been found to have potentially adverse effects on human health and the environment, or they may be ineffective in the presence of organic matter. Chlorination and ozonation may generate carcinogenic byproducts of disinfection such as trihalomethanes (THMS) and bromate. The disadvantage of UV irradiation is its lack of long-term bacteriostatic effect and the possibility of photoreactivation or dark repair of UV-damaged microorganisms, which enables regrowth of the microbial population under certain conditions (*1–6*). Recently, increasing attention has been given to reactive oxygen species (ROS), such as •OH, H_2O_2, and $•O_2^-$, which not only render cells nonviable but can also completely oxidize the bacterial components remaining after the bacteria have been killed (*1, 5–9*). The most attractive advantage of ROS, especially •OH, is their high bactericidal efficiency against almost all kinds of microorganisms (*9, 10*), which occurs without the generation of secondary pollutants. This is noticeable for TiO_2-based photocatalysts, which show effective production of ROS when applied in water disinfection. However, this technology requires the use of a relatively complex device and photo energy. The Fenton or photo-Fenton reaction system (which results from the combination of Fe^{2+} and H_2O_2) provides a promising alternative because of its ease of operation. Compared with molecular oxygen, however, the relatively high cost of H_2O_2 severely hinders its widespread application (*11*). Therefore, it is important to develop methods of catalytic disinfection by molecular oxygen that work at room temperature. Although several researchers have recently reported the catalytic oxidation of organic compounds by molecular oxygen over heterogeneous catalysts (*11, 12*), this nonphotocatalysis procedure has not been reported for treatment of drinking water.

Our previous work has shown the efficiency of Ag/Al_2O_3 and Cu/Al_2O_3 in inactivation of SARS coronavirus, *Escherichia coli*, and yeast (*5, 6*). These microbes can be completely inactivated within 5 min on an Ag/Al_2O_3 surface at room temperature in air. We have proposed a catalytic oxidation mechanism: ROS are formed as a bactericide on the catalyst surface by the activation of adsorbed oxygen during the bactericidal process (*5, 6*). When Ag/Al_2O_3 is used in water, the elution of Ag^+ from the catalyst to water is a problem. Therefore, $AlPO_4$, which is well-known to be an excellent material for adsorption and ion exchange (*13–15*), was used as the carrier in the present study, with the expectation that it would decrease the elution of Ag^+. In addition, the oxygen content in water is insufficient for the catalytic process, unlike that in air. Cerium oxide has traditionally been used as an oxygen storage material in the so-called "three-way catalysts" (TWCs) employed for the elimination of pollutants in automobile exhausts (*16–19*), and it acts as an efficient promoter to enhance the catalytic activity for oxidation of organic compounds (*20, 21*). Therefore, we prepared a silver-loaded aluminum phosphate (Ag/$AlPO_4$) catalyst with the addition of cerium and studied its bactericidal activity and mechanism using *E. coli* as an indicator bacterium.

Experimental Section

Materials. The reagent 5,5-dimethyl-1-pyrroline-*N*-oxide (DMPO) used as the spin-trapping agent in the ESR studies, and the reagent catalase used as the scavenger for H_2O_2 were purchased from the Sigma Chemical Co. and stored at −20 °C. *Escherichia coli* K12 (*E. coli* ATCC8099) was purchased from the Institute of Microbiology, Chinese Academy of Sciences. All other chemicals were of analytical grade. Deionized water was used throughout this study.

Preparation of the Catalyst. Cerium incorporated Ag/$AlPO_4$ (Ag 4 wt %) was prepared by an impregnation method. A proper amount of aluminum hydroxide powder was added slowly to a phosphoric acid solution of approximately 1 mol/L at 40–60 °C with vigorous stirring. When the reaction finished, the slurry was allowed to cool to room temperature. Silver nitrate and cerium nitrate solutions of the corresponding concentrations were then added to the slurry and mixed thoroughly by vigorous stirring. This was followed by evaporation to dryness in a rotary evaporator at 60 °C under reduced pressure. The resulting paste was dried at 120 °C for 12 h and then calcined in air at 450 and 600 °C for 3 h in sequence. Finally, the solid was ground to powder with an agate mortar and sieved into 40–60 mesh. A range of Ag(*x*Ce)/$AlPO_4$ catalysts, in which *x* denotes the molar ratio of Ce/Ag (ranging from 0.5 to 4), was obtained.

* Corresponding author phone: +86-10-62849123; fax: +86-10-62923563; e-mail: honghe@rcees.ac.cn.

[†] Research Center for Eco-Environmental Sciences, Chinese Academy of Sciences.

[‡] Institute of Chemistry, Chinese Academy of Sciences.

10.1021/es071810e CCC: $40.75
Published on Web 01/23/2008

Characterization. Powder X-ray diffraction (XRD) patterns were obtained on a Rigaku D/max-RB automatic powder X-ray diffractometer (Japan) using Cu Kα radiation at a scan rate of 6 deg (2θ) min^{-1}. These were used to identify the phase constitutions in the samples. The accelerating voltage and the applied current were 40 kV and 100 mA, respectively.

X-ray photoelectron spectroscopy (XPS) measurements were performed on a Thermo ESCALAB 250 spectrometer (Vacuum Generators, USA) using Al Kα radiation ($h\nu = 1486.6$ eV) with a constant pass energy of 20 eV. Charging effects were corrected by referencing C1s measurements at 284.8 eV. Electron spin resonance (ESR) spectra were obtained using a Bruker model ESP 300E ESR spectrometer. The settings for the ESR spectrometer wereas follows: center field 3480.00 G, microwave frequency 9.75 GHz, and power 20.15 mW.

Culture of Microorganisms. *E. coli* K12 strain ATCC8099 was inoculated into lactose broth (LB) (Fluka Co. 61748, Switzerland) and cultured aerobically for 24 h at 37 °C with constant agitation. Aliquots of the culture were inoculated into fresh medium and incubated at 37 °C for 4–5 h until they reached the exponential growth phase. Bacterial cells were collected using centrifugation at 10 000 rpm for 10 min, and then the pellet was washed and resuspended with sterilized water. Finally, bacterial cells were diluted with sterilized water and immediately plated on LB agar plates. The colonies were counted after incubation at 37 °C for 24 h. The cell density corresponding to 10^8−10^9 colony forming units per milliliter (CFU/ml) was then achieved.

Test of Bactericidal Activity. One milliliter of the *E. coli* suspension was injected into 100 mL of sterilized water, and then the prepared catalyst was added to the system. The final catalyst concentration was adjusted to 100 mg/L, and the final bacterial cell concentration was 5×10^6 CFU/mL. The reaction mixture was stirred (380 rpm) with a magnetic stirrer to prevent settling of the catalyst. All materials used in the experiments were autoclaved at 121 °C for 20 min to ensure sterility. Bacterial suspensions without any catalyst or with only the $AlPO_4$ host were used as controls. At timed intervals of 1, 10, 20, 30, and 120 min after the addition of the catalyst, 0.5 mL of the bacterial suspension without the catalyst was withdrawn and immediately diluted 10-fold in series with 4.5 mL of 0.9% saline solution (to eliminate the effect of eluted Ag^+) and plated on LB agar (Fluka Co.61746) plates. Viable cell counts were determined visually as the number of colonies per plate in serial 10-fold dilutions after incubation at 37 °C for 24 h. The reaction temperature was maintained at 25 °C. All experiments were repeated in triplicate.

Transmission electron microscopy (TEM) was used to give an insight into the size, structure, and morphology of the bacteria and particles. To avoid possible damage caused by specimen preparation, involving the procedures for fixing and embedding sensitive biological samples (*22*), native *E. coli* or a suspension of a treated sample was dropped onto copper grids with perforated carbon film, then allowed to dry in air at ambient temperature and examined using a Hitachi H-7500 TEM operated at a 60 kV accelerating voltage.

Quantitative Analysis of Silver Ions. Quantitative analysis of silver ions eluted from the catalyst in the treated suspensions was carried out by ICP-AES (inductively coupled plasma atomic emission spectrometry) analysis using an OPTIMA 2000 (Perkin-Elmer Co.). A sample (1.5 mL) of catalyst suspension with a concentration of 100 mg/L was withdrawn and filtered through a Millipore filter (pore size 0.22 μm), at each time interval, for ICP-AES analysis. All the solutions were prepared using ultrapure water in this experiment. All the above experiments were repeated in triplicate.

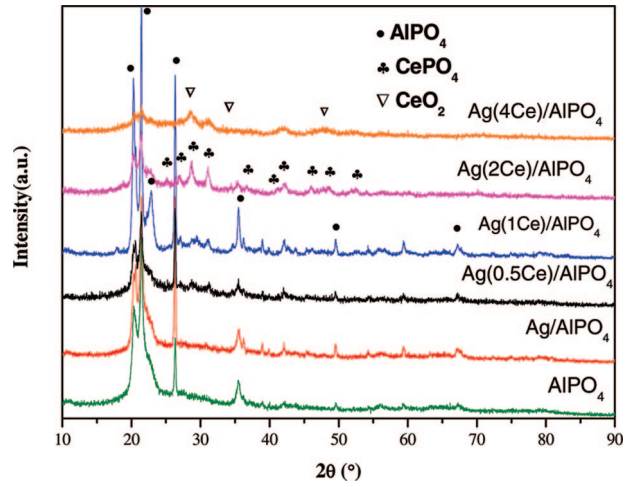

FIGURE 1. XRD patterns of $AlPO_4$ and Ag-loaded catalysts.

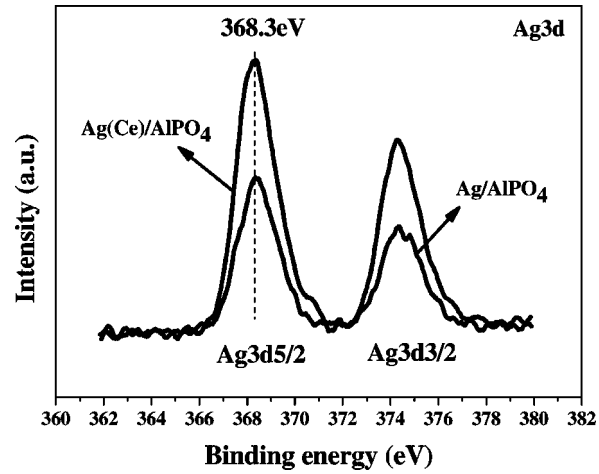

FIGURE 2. Ag3d XPS spectra of $Ag/AlPO_4$ and $Ag(Ce)/AlPO_4$ catalysts.

Results and Discussion

X-ray Diffraction Spectroscopy. The XRD patterns of Ag(*x*Ce)/$AlPO_4$ and $Ag/AlPO_4$ catalysts are shown in Figure 1. $AlPO_4$ is the main phase in the $AlPO_4$ and $Ag/AlPO_4$ catalysts. New phases representing $CePO_4$ and CeO_2 were found, and the peak intensity of $CePO_4$ and CeO_2 increased with increasing Ce content. CeO_2 was the predominant phase when the Ce/Ag ratio was higher than 4, while the principal peaks of the $AlPO_4$ phase disappeared. This indicates that the $AlPO_4$ support was completely destroyed by the addition of Ce at about 20 wt %, which probably resulted from the formation of a solid solution structure during calcination. No peaks of silver or oxide silver species were observed for any of the catalysts. The absence of diffraction lines of the silver phase on the catalyst indicates that silver is at a very high degree of dispersion on the surface of the support. Because both the structure of the $AlPO_4$ support and CeO_2 can coexist and may interact with each other or with Ag species in the catalytic process, the catalyst with a Ce/Ag ratio equal to 1 was determined to be optimum in this study for the bactericidal assay.

To determine the state of the highly dispersed Ag species in the $Ag(Ce)/AlPO_4$ catalyst, Ag3d binding energy (BE) was measured using X-ray photoelectron spectroscopy (XPS).

Figure 2 shows the XPS spectra of Ag3d in the $Ag/AlPO_4$ and Ag(Ce)/AlPO4 catalysts. The binding energy of the $Ag3d_{5/2}$ peak was located at 368.3 eV in both of the catalysts, indicating that the loaded silver is mainly in a metallic state (*23*). This result suggests that the addition of Ce has little effect on the

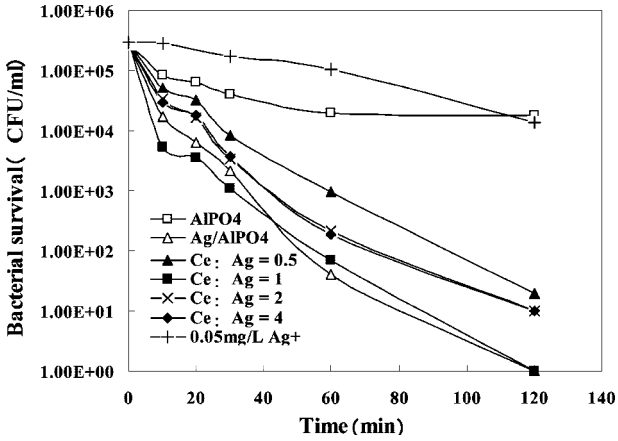

FIGURE 3. Bactericidal activity of different catalysts against *E. coli* at room temperature: catalyst concentration, 100 mg/L; initial bacterial concentration, 5 $\times 10^5$ CFU/mL.

state of the surface silver species. On the other hand, it was observed that the intensity of the $Ag3d_{5/2}$ peak of Ag(Ce)/$AlPO_4$ was much stronger than that in Ag/$AlPO_4$, indicating that coloading of Ce encourages the metallic silver to be at a much higher degree of dispersion on the surface of the support.

Bactericidal Activity against *E. coli*. The bactericidal activities of the samples were evaluated by the inactivation of *E. coli* in deionized water at room temperature, assessed on the basis of the decrease in the number of colonies of *E. coli* formed on an agar plate.

Figure 3 shows the changes in survival of *E. coli* cells on Ag(Ce)/$AlPO_4$, compared with the $AlPO_4$ support and other silver-loaded catalysts. Obvious changes in survival were not observed on the $AlPO_4$ support: a decrease of only 1.0 log unit occurred in 120 min, probably because of the adsorption function of the support, as previously reported (*13–16*). In contrast, dramatic decreases in the survival of *E. coli* cells were clearly observed when the Ag-loaded catalysts were used. Both the Ag(Ce)/$AlPO_4$ and Ag/$AlPO_4$ catalysts exhibited the strongest bactericidal activity; complete inactivation could be achieved in 120 min. A Ce/Ag ratio either above or below 1 inhibited the bactericidal activity, compared with Ag/$AlPO_4$. Therefore, the loaded silver and cerium probably interact with each other, the support, or both resulting in the existence of an optimum Ce/Ag ratio for bactericidal activity of the catalyst.

It is well-known that Ag^+ in high concentrations exhibits bactericidal activity (*24–27*), and Ag^+ elution from Ag-loaded catalysts cannot be avoided under experimental conditions. To clarify whether the Ag^+ eluted from the catalyst was the dominant factor responsible for the bactericidal activity, a quantitative analysis of Ag^+ ions eluted from the catalyst into deionized water was performed using ICP-AES. The eluted Ag^+ concentrations measured for various specimens after different periods in water with vigorous stirring are shown in Table 1.

As can be seen from the table, the concentration of Ag^+ eluted from Ag/$AlPO_4$ without addition of Ce was 0.185 mg/L in 3 h. With the Ce/Ag ratio increased to 4, the concentration of eluted Ag^+ decreased to 0.032 mg/L, indicating that the Ce co-loading reduced the speed of elution of silver. It is worthwhile to point out that the amount of Ag^+ eluted from Ag(1Ce)/$AlPO_4$ was much less than that from Ag/$AlPO_4$; however, they exhibited almost the same degree of bactericidal activity, as shown in Figure 3. Furthermore, Ag^+ at a concentration of 0.05 mg/L showed almost no bactericidal activity within 3 h (Figure 3), while the concentration of Ag^+ eluted from Ag(1Ce)/$AlPO_4$ was less than 0.05 mg/L within 3 h. Although the reason why the elution of Ag^+ was inhibited

TABLE 1. Concentration of Eluted Ag^+ from Different Catalysts in Deionized Water

	concentration of eluted Ag^+ (mg/L)		
catalyst	1 h	2 h	3 h
Ag/$AlPO_4$	0.110	0.127	0.185
Ag(0.5Ce)/$AlPO_4$	0.063	0.102	0.129
Ag(1Ce)/$AlPO_4$	0.027	0.038	0.048
Ag(2Ce)/$AlPO_4$	0.017	0.027	0.036
Ag(4Ce)/$AlPO_4$	0.015	0.023	0.032

by the addition of Ce is still unclear, these results clearly suggest that the toxicity of Ag^+ did not play an important role in the inactivation of *E. coli* by Ag(Ce)/$AlPO_4$. The synergistic effect of Ag^+ with some reactive oxygen species (ROS), promoted by coloading of Ce, may evolve during the bactericidal process (*8, 28*).

Transmission Electron Microscopy Imaging. To further clarify whether the bactericidal effect was caused by Ag^+, TEM was used to directly observe the morphological changes in the *E. coli* cells after treatment by the catalysts or Ag^+ in deionized water. Figure 4a shows a TEM image of untreated *E. coli* cells. The cells were glossy and plump and showed uniform electron density, suggesting that the cells were in a normal condition without environmental disturbance.

Dramatic morphological changes occurred in *E. coli* cells after Ag(Ce)/$AlPO_4$ treatment for 0.5 h, as shown in Figure 4b. The *E. coli* cells swelled to a much greater size than the untreated cells (see Figure 4a) and were no longer rod shaped. Moreover, the cell envelope of the *E. coli* cells was significantly damaged, resulting in leakage of the intracellular constituents; therefore some electron-lucent regions appeared. Following

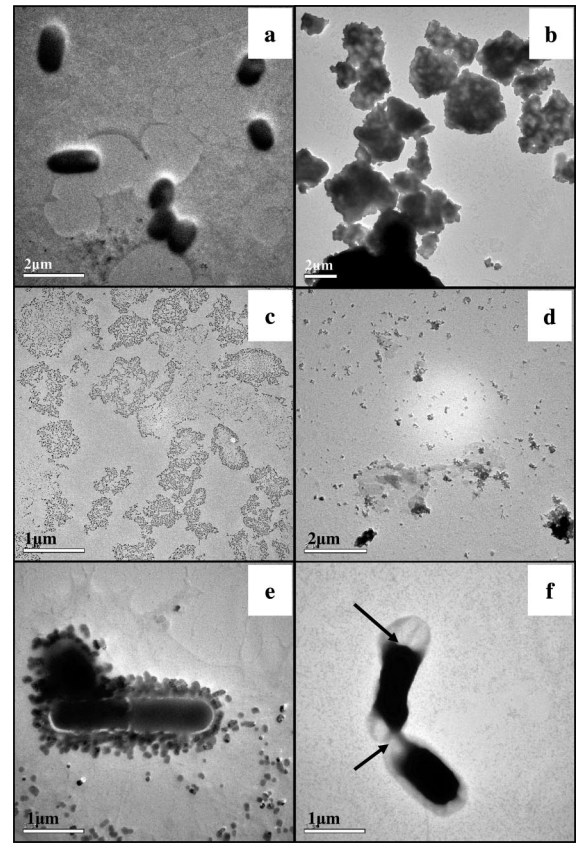

FIGURE 4. TEM images of (a) untreated *E. coli* cells and *E. coli* cells (b) treated with Ag(Ce)/$AlPO_4$ in deionized water for 0.5 h, (c) 2 h, (d) 3 h; treated with (e) 0.5 mg/L Ag^+, and (f) 1 mg/L Ag^+ in deionized water for 3 h at room temperature.

longer treatment by the catalyst, around 2–3 h, whole cells completely disappeared; finally, nothing was observed but a large number of destroyed cell fragments, as shown in Figure 4c and d.

In contrast, the *E. coli* cells treated with 0.5 and 1 mg/L of Ag^+ (shown in Figure 4e and f) under the same conditions exhibited very different morphological changes during the process of inactivation. A considerable amount of large electron-dense granules were observed around the cell wall after treatment with 0.5 mg/L Ag^+ for 3 h (Figure 4e). Feng et al. (*26*) reported that it is possible that some of the stimulated proteins produced by the cells conglomerate after attack with silver ions and surround the cell wall to protect the *E. coli* cells from further destruction. After treatment with 1 mg/L of Ag^+, the cytoplasm of the *E. coli* cells obviously shrank, and a large gap appeared between the cytoplasmic membrane and the cell wall (arrow in Figure 4 (f)). It should be noted that all the silver treated cells were still homogeneous, and no electron-lucent regions appeared at either of the concentrations. The same phenomenon was observed by Yamanaka et al. (*22*), and these authors proposed that the Ag^+ penetrated into the interior of the cell through ion channels without causing damage to the cell membranes. Feng et al. (*26*) also reported that Ag^+ were detected inside the *E. coli* cells by EDAX, indicating an interaction with thiol groups in cytoplasmic proteins that led to the inactivation of the bacterial proteins.

The concentrations of Ag^+ used in this study were much higher than those of Ag^+ eluted from the catalyst because lower concentrations of Ag^+ would cause only minor morphological changes of *E. coli* cells that could not be observed by TEM. The quite different morphological changes of *E. coli* cells treated with the $Ag(Ce)/AlPO_4$ catalyst and those treated with Ag^+ clearly imply two different bactericidal mechanisms. It can be deduced that $Ag(Ce)/AlPO_4$ catalyzed the formation of ROS, which are more active in destroying the *E. coli* cells. Indeed, silver-loaded catalysts are well-known for exhibiting catalytic activity (*8, 9, 11, 28–30*), and the addition of Ce is thought to promote oxidative activity because of its high oxygen storage capability (OSC), allowing release of oxygen in a reducing environment and uptake of oxygen in an oxidizing environment (*16, 18*). Because oxygen has been reported to play an important role in the formation of ROS (*5–9, 11, 28*) on the catalyst surface, it may be mainly responsible for the strong bactericidal activity demonstrated. To investigate the ROS formed on the catalyst surface, electron spin resonance spectroscopy (ESR) was used to obtain the information on $^{\bullet}OH$ and $^{\bullet}O_2^-$, the typical ROS formed during catalytic oxidation.

Electron Spin Resonance Spectroscopy. The ESR spin-trap technique, using 5, 5-dimethyl-1-pyrroline-*N*-oxide (DMPO) as the spin-trapping reagent, is well-known to be an efficient measurement method to determine $^{\bullet}OH$ and $^{\bullet}O_2^-$ radicals (*1, 11, 31, 32*). Because the $^{\bullet}O_2^-$ radicals in water are very unstable and undergo facile disproportionation rather than slow reaction with DMPO (*31, 32*), the involvement of $^{\bullet}O_2^-$ radicals was examined in methanol. Figure 5 illustrates the ESR spectra of the DMPO−$OH^{\bullet}$ spin adduct and DMPO−$O_2^{-\bullet}$ spin adduct measured immediately after mixing of the catalyst with DMPO solution at room temperature.

As shown in Figure 5a and b, no signals were detected before the addition of the $Ag(Ce)/AlPO_4$ catalyst in aqueous dispersion, and the four characteristic peaks of the DMPO−$OH^{\bullet}$ species, a 1:2:2:1 quartet pattern, were clearly observed after the addition of the catalyst. Similarly, the six characteristic peaks of the DMPO−$O_2^{-\bullet}$ adducts were also observed only in the presence of $Ag(Ce)/AlPO_4$ in methanol dispersion, as shown in Figure 5c and d. However the signals of DMPO−$O_2^{-\bullet}$ were obviously weaker than those of DMPO−$OH^{\bullet}$. These results suggest that $^{\bullet}OH$ and $^{\bullet}O_2^-$ were

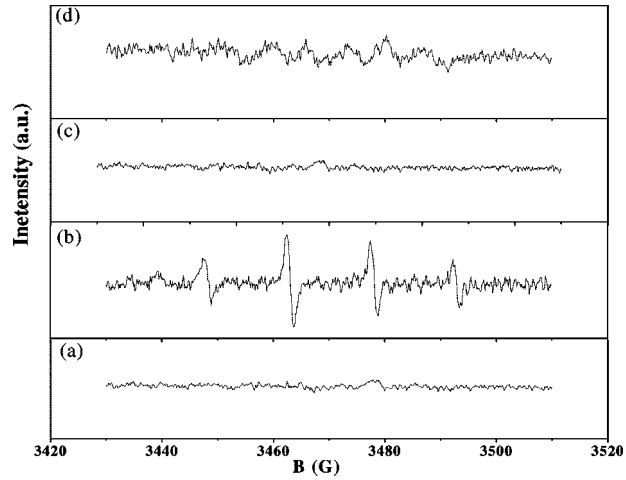

FIGURE 5. DMPO spin-trapping ESR spectra recorded at ambient temperature in aqueous dispersion (for DMPO−$OH^{\bullet}$ adduct) (a) before and (b) after the addition of $Ag(Ce)/AlPO_4$ catalyst, in methanol dispersion (for DMPO−$O_2^{-\bullet}$ adduct) (c)before and (d) after the addition of $Ag(Ce)/AlPO_4$ catalyst.

both produced on the catalyst surface, and $^{\bullet}OH$ may be mainly responsible for the catalytic oxidation of the *E. coli* cells. The evidence that $^{\bullet}OH$ and $^{\bullet}O_2^-$ are formed on the surface of the $Ag(Ce)/AlPO_4$ catalyst provides a solid indication that the catalyst can efficiently activate the adsorbed oxygen to produce a series of active oxygen radicals, which finally induces the decomposition of the bacteria (*31*).

Effect of ROS In the Bactericidal Process. The formation of the reactive radicals in the solution is thought to depend mainly on the high oxygen storage capability of surface ceria, which are well-known for their excellent ability to activate/store oxygen and transform/release oxygen species, resulting from the redox cycle of Ce^{3+}/Ce^{4+} (*16, 18, 20, 22, 33*). Therefore, oxygen molecules dissolved in water could be introduced into the reaction system through the redox cycle of Ce^{3+}/Ce^{4+}, and activated to the chemisorbed oxygen. Furthermore, as previously reported (*8, 34*), once Ag is dispersed as metal particles on porous oxide, the finely divided Ag particle surface may have sufficient defects for dissociative chemisorption of oxygen and enhance the catalytic oxidation activity to hydrocarbon oxidation. Therefore, the chemisorbed oxygen would be supplied to the silver nearby, maintaining the recycling of the oxidative state of the silver.

Accordingly, consecutive oxygen transfer steps from the oxygen reservoir Ce^{3+}/Ce^{4+} to the Ag active site, being activated to ROS, is proposed as follows:

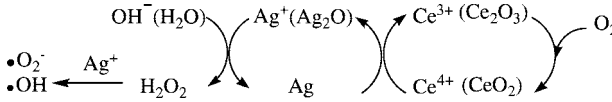

To our knowledge, φ^{θ} $Ce^{4+}/Ce^{3+} = 1.61V$, φ^{θ} $Ag^+/Ag = 0.80V$, φ^{θ} $HO_2^-/OH^- = 0.695V$; therefore, this mechanism is theoretically reasonable, and the electron-transfer process can carry through the successive steps. Thomas and coworkers demonstrated highly selective oxidation of *n*-alkanes at the terminal carbon atoms, using molecular oxygen over microporous aluminum phosphates in which Mn or Co species were introduced into the framework as redox centers, with a similar mechanism (*12*). This mechanism could also give a good explanation for the existence of an optimal Ce/Ag ratio for electron transfer.

In addition, the bactericidal activity of $Ag(Ce)/AlPO_4$ increased with increasing pH (data not shown), which strongly supports the proposed catalytic bactericidal mech-

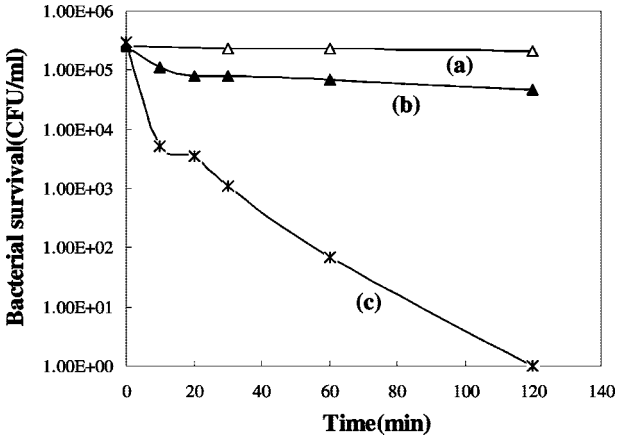

FIGURE 6. Effect of catalase against H_2O_2 on the bactericidal activity of Ag(Ce)/$AlPO_4$ at room temperature: (a) blank, (b) 286 units/mL catalase + 100 mg/L Ag(Ce)/$AlPO_4$, (c) 100 mg/L Ag(Ce)/$AlPO_4$. Initial bacterial concentration: 5×10^5 CFU/mL.

anism. The formation of H_2O_2 has already been shown for other silver-loaded catalysts in water (*8, 28*) and was also confirmed in our study by addition of catalase as the scavenger of H_2O_2 (Figure 6).

As can be seen from Figure 6, with the addition of 286 units/mL catalase, the bactericidal activity of the catalyst was inhibited dramatically. This result indicates that the formation of H_2O_2 plays an important role during the bactericidal process. The addition of catalase has two effects (*8*): transformation of H_2O_2 to water as described by the chemical equation $2H_2O_2$ + catalase $\rightarrow$ O_2 + $2H_2O$ and interception of the route of formation of $^{\bullet}OH$ because $^{\bullet}OH$ is formed by the decomposition of H_2O_2. As previously reported (*8, 28, 34*), transitional metals such as silver and ferrous ions can catalyze the oxidizing action of H_2O_2 by forming $^{\bullet}OH$, $^{\bullet}O_2^-$, or both through a so-called Fenton-like reaction. As a result, $^{\bullet}OH$ and other ROS, such as $^{\bullet}O_2^-$ and H_2O_2, simultaneously contribute to the efficient inactivation of *E. coli* cells.

In conclusion, molecular oxygen catalyzed by an Ag(Ce)/$AlPO_4$ catalyst exhibited good bactericidal activity against *E. coli* cells, resulting from the high oxygen storage capability of surface ceria and desirable dispersion of Ag particles on the catalyst surface. ROS with strong oxidative properties, such as $^{\bullet}OH$ and $^{\bullet}O_2^-$, were successfully detected by ESR at room temperature without extra light or electric power input, which provides direct evidence for the catalytic inactivation of *E. coli* cells by the Ag(Ce)/$AlPO_4$ catalyst using molecular oxygen. The formation of H_2O_2 as an important intermediate was confirmed by addition of catalase, thus strongly supported the proposed catalytic oxidation mechanism. This may provide a novel approach for the efficient disinfection of drinking water. Further study of the interaction of surface metal species and ROS with bacteria on the catalyst surface is currently in progress.

Acknowledgments

This work was financially supported by the National Natural Science Foundation of China (50621804, 50538090) and the Ministry of Science and Technology, China (2007CB407301).

Literature Cited

(1) Yu, J. C.; Ho, W.; Yu, J.; Yip, H.; Wong, P. K.; Zhao, J. Efficient visible-light-induced photocatalytic disinfection on sulfur-doped nanocrystalline titania. *Environ. Sci. Technol.* **2005**, *39*, 1175–1179.

(2) Koivunen, J.; Heinonen-Tanski, H. Inactivation of enteric microorganisms with chemical disinfectants, UV irradiation and combined chemical/UV treatments. *Water Res.* **2005**, *39*, 1519–1526.

(3) Ince, N. H.; Belen, R. Aqueous phase disinfection with power ultrasound: Process kinetics and effect of solid catalysts. *Environ. Sci. Technol.* **2001**, *35*, 1885–1888.

(4) Dadjour, M. F.; Ogino, C.; Matsumura, S.; Shimizu, N. Kinetics of disinfection of *Escherichia coli* by catalytic ultrasonic irradiation with TiO_2. *Biochem. Eng. J.* **2005**, *25*, 243–248.

(5) He, H.; Dong, X.; Yang, M.; Yang, Q.; Duan, S.; Yu, Y.; Han, J.; Zhang, C.; Chen, L.; Yang, X. Catalytic inactivation of SARS, coronavirus, *Escherichia coli* and yeast on solid surface. *Catal. Commun.* **2004**, *5*, 170–172.

(6) Chen, M.; Yan, L.; He, H.; Chang, Q.; Yu, Y.; Qu, J. Catalytic sterilization of *Escherichia coli* K12 on Ag/Al_2O_3 surface. *J. Inorg. Biochem.* **2007**, *101*, 817–823.

(7) Sunada, K.; Kikuchi, Y.; Hashimoto, K.; Fujishima, A. Bactericidal and detoxification effects of TiO_2 thin film photocatalysts. *Environ. Sci. Technol.* **1998**, *32*, 726–728.

(8) Inoue, Y.; Hoshino, M.; Takahashi, H.; Noguchi, T.; Murata, T.; Kanzaki, Y.; Hamashima, H.; Sasatsu, M. Bactericidal activity of Ag−zeolite mediated by reactive oxygen species under aerated conditions. *J. Inorg. Biochem.* **2002**, *92*, 37–42.

(9) Jeong, J.; Kim, J. Y.; Yoon, J. The role of reactive oxygen species in the electrochemical inactivation of microorganisms. *Environ. Sci. Technol.* **2006**, *40*, 6117–6122.

(10) Cho, M.; Lee, Y.; Chung, H.; Yoon, J. Inactivation of *Escherichia coli* by photochemical reaction of ferrioxalate at slightly acidic and near-neutral pHs. *Appl. Environ. Microbiol.* **2004**, *70* (2), 1129–1134.

(11) Meng, X.; Lin, K.; Yang, X.; Sun, Z.; Jiang, D.; Xiao, F. S. Catalytic oxidation of olefins and alcohols by molecular oxygen under air pressure over $Cu_2(OH)PO_4$ and $Cu_4O(PO_4)_2$ catalysts. *J. Catal.* **2003**, *218*, 460–464.

(12) Thomas, J. M.; Raja, R; Sankar, G.; Bell, R. G. Molecular-sieve catalysts for the selective oxidation of linear alkanes by molecular oxygen. *Nature* **1999**, *398*, 227–230.

(13) Campelo, J. M.; Jaraba, M.; Luna, D.; Luque, R.; Marinas, J. M.; Romero, A. A. Effect of phosphate precursor and organic additives on the structural and catalytic properties of amorphous mesoporous $AlPO_4$ Materials. *Chem. Mater.* **2003**, *15*, 3352–3364.

(14) Takita, Y.; Wakamatsu, H.; Li, G. L.; Yoshihiko, M.; Nishiguchi, H.; Tatsumi, I. Decomposition of chlorofluorocarbons over metal phosphate catalysis II: Origin of the stability of $AlPO_4$ and the location of Ce as a promoter. *J. Mol. Catal. A: Chem.* **2000**, *155*, 111–119.

(15) Kunio, K.; Kazumichi, S.; Akitsugu, O. Morphology of aluminum phosphate by the Al−EDTA mediated particle formation in aqueous solutions at high temperatures. *Mater. Res. Bull.* **2007**, *42*, 256–264.

(16) Martínez-Arias, A.; Fernández-García, M.; Salamanca, L. N.; Valenzuela, R. X.; Conesa, J. C.; Soria, J. Structural and redox properties of ceria in alumina-supported ceria catalyst supports. *J. Phys. Chem. B.* **2000**, *104*, 4038–4046.

(17) Scott, A. H.; Steven, S. C. C.; Khalid, A.; Robert, W. S., Jr. Transient infrared characterization of oxygen storage capability of Ce−Pd/Al_2O_3 catalyst during NO−CO reaction. *J. Phys. Chem. B.* **2003**, *107*, 4834–4843.

(18) Aboukais, A.; Zhilinskaya, E. A.; Lamonier, J. F.; Filimonov, I. N. EPR study of ceria−silica and ceria−alumina catalysts: Localization of superoxide radical anions. *Colloids Surf., A* **2005**, *260*, 199–207.

(19) Martínez-Arias, A.; Coronado, J. M.; Cataluña, R.; Conesa, J. C.; Soria, J. Influence of mutual platinum-dispersed ceria interactions on the promoting effect of ceria for the CO oxidation reaction in a Pt/CeO_2/Al_2O_3 catalyst. *J. Phys. Chem. B* **1998**, *102*, 4357–4365.

(20) Yang, S.; Feng, Y.; Wan, J.; Zhu, W.; Jiang, Z. Effect of CeO_2 addition on the structure and activity of RuO_2/γ-Al_2O_3 catalyst. *Appl. Surf. Sci.* **2005**, *246*, 222–228.

(21) Zhang, X.; Wan, H.; Weng, W. Z.; Yi, X. D. Effect of promoter Ce on silver−molybdenum−phosphate catalysts for selective oxidation of propane to acrolein. *J. Mol. Catal. A: Chem.* **2003**, *200*, 291–300.

(22) Yamanaka, M.; Hara, K.; Kudo, J. Bactericidal actions of a silver ion solution on *Escherichia coli*, studied by energy-filtering transmission electron microscopy and proteomic analysis. *Appl. Environ. Microbiol.* **2005**, *71*, 7589–7593.

(23) Onodera, Y.; Iwasaki, T.; Chatterjee, A.; Ebina, T.; Satoh, T.; Suzuki, T.; Mimura, H. Bactericidal allophanic materials prepared from allophane soil I. Preparation and characterization of silver−phosphorus−silver loaded allophanic specimens. *Appl. Clay Sci.* **2001**, *18*, 123–134.

(24) Sökmena, M.; Candan, F.; Sümer, Z. Disinfection of *E. coli* by the Ag−TiO_2/UV system: Lipidperoxidation. *J. Photochem. Photobio. A.* **2001**, *143*, 241–244.
(25) Davies, R. L.; Etris, S. F. The development and functions of silver in water purification and disease control. *Catal. Today.* **1997**, *36*, 107–114.
(26) Feng, Q. L.; Wu, J.; Chen, G. Q.; Cui, F. Z.; Kim, T. N.; Kim, J. O. A mechanistic study of the antibacterial effect of silver ions on *Escherichia coli* and *Staphylococcus aureus*. *J. Biomed. Mater. Res. A.* **2000**, *52*, 662–668.
(27) Yoshinobu, M.; Kuniaki, Y.; Shin-ichi, K.; Tetsuaki, T. Mode of bactericidal action of silver zeolite and its comparison with that of silver nitrate. *Appl. Environ. Microbiol.* **2003**, *69*, 4278–4281.
(28) Pape, H. L.; Solano-Serena, F.; Contini, P.; Devillers, C.; Maftah, A.; Leprat, P. Involvement of reactive oxygen species in the bactericidal activity of activated carbon fibre supporting silver-bactericidal activity of ACF(Ag) mediated by ROS. *J. Inorg. Biochem.* **2004**, *98*, 1054–1060.
(29) Wu, Q.; Gao, H.; He, H. Conformational analysis of sulfate species on Ag/Al_2O_3 by means of theoretical and experimental vibration spectra. *J. Phys. Chem. B* **2006**, *110*, 8320–8324.
(30) Yu, Y.; He, H.; Feng, Q.; Gao, H.; Yang, X. Mechanism of the selective catalytic reduction of NOx by C_2H_5OH over Ag/Al_2O_3. *Appl. Catal., B* **2004**, *49*, 159–171.
(31) Hu, C.; Hu, X.; Guo, J.; Qu, J. Efficient destruction of pathogenic bacteria with NiO/$SrBi_2O_4$ under visible light irradiation. *Environ. Sci. Technol.* **2006**, *40* (17), 5508–5513.
(32) Ma, W.; Huang, Y.; Li, J.; Cheng, M.; Song, W.; Zhao, J. An efficient approach for the photodegradation of organic pollutants by immobilized iron ions at neutral pHs. *Chem. Commun.* **2003**, 1582–1583.
(33) Zhang, X.; Wan, H.; Weng, W.; Yi, X. Effect of promoter Ce on silver−molybdenum−phosphate catalysts for selective oxidation of propane to acrolein. *J. Mol. Catal. A: Chem.* **2003**, *200*, 291–300.
(34) Zhang, L.; Yu, J. C.; Yip, H. Y.; Li, Q.; Kwong, K. W.; Xu, A. W.; Wong, P. K. Ambient light reduction strategy to synthesize silver nanoparticles and silver-coated TiO_2 with enhanced photocatalytic and bactericidal activities. *Langmuir* **2003**, *19*, 10372–10380.

ES071810E